Journal of NeuroVirology, 12: 262–271, 2006

ISSN: 1355-0284 print / 1538-2443 online
DOI: 10.1080/13550280600873868

informa
healthcare

Positron emission tomography imaging of peripheral benzodiazepine receptor binding in human immunodeficiency virus–infected subjects with and without cognitive impairment

Clayton A Wiley,[1] Brian J Lopresti,[2] James T Becker,[3,4,5] Fernando Boada,[2] Oscar L Lopez,[3,4] John Mellors,[6] Carolyn C Meltzer,[7,8] Stephen R Wisniewski,[9] and Chester A Mathis[2]

Departments of [1]Pathology, [2]Radiology, [3]Psychiatry, [4]Neurology, [5]Psychology, and [6]Medicine, University of Pittsburgh School of Medicine, Pittsburgh, Pennsylvania, USA; Departments of [7]Radiology and [8]Neurology, Emory University School of Medicine, Atlanta, Georgia, USA; [9]Department of Epidemiology, University of Pittsburgh Graduate School of Public Health, Pittsburgh, Pennsylvania, USA

The pathology associated with late-stage dementia in human immunodeficiency virus (HIV) infection has been studied extensively. Neuropathological examination has demonstrated abundant activation and infection of macrophages/microglia termed HIV encephalitis. For obvious reasons, less is known regarding the neuropathology of minor cognitive impairment seen in earlier stages of HIV infection. The authors examined the utility of the peripheral benzodiazepine receptor ligand PK11195 in positron emission tomography (PET) imaging to assess microglial/macrophage activation in the brains of HIV-infected subjects with minor neurocognitive impairment in a cross-sectional study of 12 HIV infected individuals and 5 age-matched noninfected controls. Subjects were given a battery of neuropsychological tests in addition to assessing CD4 T-cell count and peripheral viremia followed by contrast enhanced magnetic resonance imaging (MRI) and PET with [^{15}O]H_2O followed by [^{11}C](*R*)-PK11195. Two of the six neurocognitively impaired HIV-infected subjects demonstrated plasma viral breakthrough, whereas only one of six nonimpaired individuals demonstrated plasma viral load near the limits of detection. MRI demonstrated no abnormal enhancement and although atrophy was more prominent in impaired subjects, it was also present though to a lesser extent in nonimpaired subjects. None of the 12 HIV-infected subjects demonstrated increased retention of [^{11}C](*R*)-PK11195 in the brain parenchyma compared to the 5 controls. These results suggest that either [^{11}C](*R*)-PK11195 PET assessment is insensitive to the degree of macrophage activation in HIV-associated minor neurocognitive impairment or macrophage activation is not the pathological substrate of this neurological condition. *Journal of NeuroVirology* (2006) **12,** 262–271.

Keywords: dementia; HIV-1–associated cognitive motor complex; macrophages; microglia; peripheral benzodiazepine receptor; positron emission tomography

Introduction

Human immunodeficiency virus (HIV)-infected individuals develop a spectrum of neurological impairments ranging from minor motor and cognitive abnormalities to frank dementia (Dal Pan and McArthur, 1996; Grant *et al*, 1995; McArthur *et al*, 2003). The etiologies and relationships among these different cognitive abnormalities are unknown. Autopsy studies have demonstrated that the pathological substrate of dementia in immunosuppressed acquired immunodeficiency syndrome (AIDS) patients without opportunistic brain infections is HIV encephalitis (Achim *et al*, 1994; Budka, 1991; Glass *et al*, 1995). Histopathological hallmarks of HIV encephalitis include abundant brain tissue infiltration

Address correspondence to Dr. Clayton A. Wiley, Presbyterian University Hospital, Neuropathology Division, 200 Lothrop Street A515, Pittsburgh, PA 15213, USA. E-mail: wileyca@upmc.edu

This work was supported by the National Institutes of Health; MH64921 (CAW), MH01717 (CAW), MH45311 (JTB), AG021431 (JTB), and MH01077 (JTB).

Received 26 April 2006; revised 26 May 2006; accepted 5 June 2006.

by macrophages, multinucleated giant cells, microglial nodules, and perivascular chronic inflammatory cells (Budka, 1991). Because HIV does not infect neuroglia to a significant degree, how HIV encephalitis leads to dementia is an enigma. Current hypotheses implicate viral proteins and toxins derived from both HIV-infected and activated macrophages that cause synaptic damage leading to cognitive dysfunction (Wiley *et al*, 1991; Masliah, 1992). Because minor cognitive abnormalities appear earlier in the disease process, prior to the development of terminal immunosuppression, our understanding of their pathological substrate is less clear and relies upon *in vivo* assessments such as brain imaging.

Several imaging modalities have been used to assess central nervous system (CNS) changes associated with lentiviral infection (Avison *et al*, 2002; Paul *et al*, 2002; Post *et al*, 1988). Although x-ray computed tomography has been considered relatively insensitive, magnetic resonance imaging (MRI) has demonstrated a spectrum of lesions, including white matter abnormalities and brain atrophy, in demented HIV-infected subjects (Aylward *et al*, 1993; McArthur *et al*, 1990; Post *et al*, 1992; Raininko *et al*, 1992; Sonnerborg *et al*, 1990; Wenserski *et al*, 2003). Functional imaging studies using positron emission tomography (PET) with the fluorine-18–labeled glucose analog [^{18}F]2-fluoro-2-deoxyglucose ([^{18}F]FDG), single-photon emission computed tomography, magnetic resonance spectroscopy, and functional MRI have offered tantalizing insights into lentiviral infection, but no definitive relationship between abnormalities and onset of neurological disease has been observed (Chang *et al*, 1999; Ernst *et al*, 2003; Pascal *et al*, 1991; Rosci *et al*, 1992). If HIV-associated CNS damage could be evaluated during life, it would help define the time course of disease and help define efficacy of therapy before development of fixed neurological deficits. Because activated and infected macrophages are the *sine qua non* of HIV encephalitis (Budka, 1991; Kaul *et al*, 2001), it may be possible to monitor the progression of HIV encephalitis if it were possible to monitor the presence of macrophages *in vivo*.

Recently radiolabeled ligands have been synthesized that selectively bind to the peripheral benzodiazepine receptor (PBR), which is abundantly expressed on activated brain macrophages (Banati, 2002; Cagnin *et al*, 2002). The isoquinoline carboxamide derivative PK11195 [1-(2-chlorophenyl)-*N*-methyl-*N*-(1-methylpropyl)-3-isoquinolinecarboxamide] is a specific ligand for PBR. Because PBR is expressed only at low levels in the normal brain, several *in vitro* and *in vivo* studies have examined whether [^{11}C]PK11195 can be used to radiolabel activated macrophages in the diseased CNS. Autoradiographic studies have demonstrated increased binding of [^{3}H]PK11195 to macrophages in a wide variety of neurological diseases such as multiple sclerosis and experimental autoimmune encephalitis (Banati *et al*, 2000; Vowinckel *et al*, 1997), stroke (Stephenson *et al*, 1995), and brain trauma (Raghavendra Rao *et al*, 2000). Several studies have utilized PET with [^{11}C]PK11195 to detect activated macrophages in the CNS of patients with multiple sclerosis (Banati *et al*, 2000; Vowinckel *et al*, 1997; Debruyne *et al*, 2003), Rasmussen's encephalitis (Banati *et al*, 1999), herpes encephlalitis (Cagnin *et al*, 2001b), Alzheimer's disease (Cagnin *et al*, 2001a), multiple system atrophy (Gerhard *et al*, 2003), and most recently early Parkinson's disease (Ouchi *et al*, 2005). We have recently used [^{11}C](***R***)-PK11195 PET in studies of the simian CD8 T-cell depletion model of HIV encephalitis and observed correlations between *in vivo* specific binding of [^{11}C](***R***)-PK11195 and necropsy evidence of lentiviral encephalitis (Venneti *et al*, 2004). During the preparation of this paper, Hammoud *et al* (2005) reported [^{11}C](***R***)-PK11195 PET in 5 healthy subjects and 10 HIV-infected subjects. They found differences in [^{11}C](***R***)-PK11195 binding between infected and noninfected subjects but not between demented and nondemented subjects.

To examine the hypothesis that minor neurocognitive changes are an early stage in HIV encephalitis and the result of microglial activation, we used gadolinium-enhanced MRI and [^{11}C](***R***)-PK11195 PET to study 12 chronic HIV-infected subjects, 6 with and 6 without neurocognitive impairment and 5 non-HIV-infected controls. MRI demonstrated no abnormal enhancement and although atrophy was more severe in the impaired subjects, it was also present in the nonimpaired subjects. None of the 12 subjects demonstrated increased retention of [^{11}C](***R***)-PK11195 in the brain parenchyma. These findings suggest that minor neurocognitive impairment occurring during HIV infection is not the result of microglial activation at a level detectable by [^{11}C](***R***)-PK11195 PET and thus potentially not a precursor of HIV dementia.

Results

Subjects

A total of 18 subjects were enrolled in the study; however, 1 subject had to be excluded from analysis because of movement during PET scanning (see Table 1). All 12 HIV-infected subjects were taking a variety of antiretroviral drugs. HIV RNA was not detectable in the plasma of 9 infected subjects, whereas the other 3 infected subjects showed varying degrees of breakthrough viremia (Table 1). There was no clear relationship between plasma viral load and CD4 T-cell count.

A summary of the neuropsychological test results are shown in Table 2. Briefly, they show that although the impaired subjects have equivalent premorbid IQs compared to the unimpaired subjects, they nevertheless showed distinct areas of impaired function. Performance on the Digit Symbol Substitution Task, an

index of psychomotor speed, visual scanning, and incidental learning, was impaired, even after expressing the raw score as an age-adjusted scaled score. Access to educationally based world knowledge and word definitions was poorer (albeit not significantly) in the impaired subjects, as was their ability to perform Block Design constructions. However, it was in the memory tests that the impaired subjects performed most poorly. They demonstrated lower delayed recall scores for both verbal and nonverbal material, and were able to recall fewer words during verbal learning. Verbal fluency was unaffected in the two patient groups. Psychomotor speed (Trailmaking A, Grooved Pegboard) was abnormally slow in the impaired patients. Psychomotor speed, as assessed by the Trailmaking Test, was slower in the impaired subjects, although fine motor coordination (Grooved Pegboard) was unaffected.

MR Imaging

MR images of the 12 HIV-infected subjects demonstrated no difference in structural abnormalities or abnormal enhancement (Table 1). Although subjective atrophy was more severe in the impaired subjects, it did not consistently distinguish between impaired and nonimpaired subjects. Because no abnormal enhancement of postcontrast scans was found, no further analysis of the dynamic contrast enhanced data sets (EPI) was performed. The studies were further assessed for neuroimaging findings described as consistent with direct HIV effects or HIV encephalopathy, including cerebral volume loss and white matter hyperintensities (Broderick *et al*, 1993; Grassi *et al*, 1997; Lexa, 1994; Olsen *et al*, 1988; Post *et al*, 1988). The pattern of volume loss is typically characterized by ventricular enlargement that is out of proportion to sulcal enlargement, accompanied by symmetric central white matter abnormalities. There is conflicting evidence as to whether these findings are related to the degree of cognitive impairment (Di Sclafani *et al*, 1997; Harrison *et al*, 1998; Patel *et al*, 2002). MRI abnormalities were more common in the impaired subjects, but one of six impaired subjects did not show any abnormalities whereas one of six nonimpaired subjects showed abnormalities, in each of the categories.

PET Imaging

Following the injection of [^{11}C](***R***)-PK11195, brain radioactivity time activity curves demonstrated significant brain uptake and rapid clearance from all brain areas. It was expected that specific binding of [^{11}C](***R***)-PK11195 would be detected as a decreased rate of clearance from regions of brain tissue that harbored populations of activated microglia. Although some regional variation in the retention characteristics were observed, no discernible component of specific binding was observed in any brain region in impaired HIV-infected subjects as compared to noninfected HIV subjects or seronegative controls (Table 3, Figure 1).

Discussion

We used MRI and PET to study a small group of HIV-infected neurocognitively impaired and nonimpaired individuals along with five noninfected control subjects. As all of our subjects received antiretroviral

Table 1 Subject age, CD4 T-cell count, viral load, and MRI findings

Subject	*Age*	*CD4 %*	*CD4 count*	*Viral load*	*Neurocognitive*	*Vent. enlarge*	*Perivent, HI*	*HIV ENC*
CW03-01	41	25	524	<50	I	+	+	+
CW03-08	52	14	528	9202	I	+	++	+
CW04-02	39	10	148	38926	I	+	++	+
CW05-04	54	11	161	<50	I	++	++	++
CW03-04	45	40	345	<50	I	−	−	−
CW04-03	53	14	376	<50	I	+	+	+
CW03-07	66	37	736	60	NI	−	+	−
CW04-01	39	36	894	<50	NI	−	−	−
CW03-02	52	19	384	<50	NI	−	−	−
CW03-05	43	29	393	<50	NI	+	+	+
CW03-06	52	24	555	<50	NI	−	+	−
CW05-02	46	43	698	<50	NI	−	−	−
Non-infected controls								
CW04-05	54	55	1211	−	C	−	−	−
CW04-06	44	51	868	−	C	−	−	−
CW04-07	27	51	1782	−	C	−	−	−
CW05-01	43	42	898	−	C	−	−	−
CW05-03	34	53	1069	−	C	−	−	−

CD4%: percentage of lymphocytes determined to be CD4 T-cells on the basis of flow cytometry; CD4 count: absolute number of CD4 T-cells per mm^3 of blood; Viral load: number of copies of HIV RNA per mm^3 of plasma; Neurocognitive: determination of neurocognitive status as impaired (I) or nonimpaired (NI) as outline in methods or control noninfected (C); Vent. enlarg.: + denotes present, − denotes absent; Perivent. HI: hyperintensities, − denotes absent, + denotes mild, ++ denotes moderate; Thin CC: corpus callosum thinning, + denotes present, − denotes; absent; HIV ENC: pattern of MRI volume loss and white matter hyperintensities consistent with subjective radiological impression of HIV encephalopathy.

Table 2 Selected neuropsychological test data

		Patients	
N	*Controls* 5	*Unimpaired* 6	*Impaired* 6
Age	43.5 (28–51)	49.5 (40–66)	48.8 (39–55)
Education	14.0 (12–18)	16.0 (14–19)	14.0 (8–18)
Estimated IQ	106 (104–108)	123 (115–126)	114 (111–129)
WAIS-R Vocabulary	10.0 (8–14)	11.0 (9–19)	11.0 (5–14)
Information	9.0 (8–14)	13.5 (9–15)	12.0 (4–13)
Block Design	14.5 (10–15)	12.0 (9–18)	9.5 (7–12)
Digit Symbol Raw Score	59.0 (46–89)	59.0 (55–67)	50.5 (34–61)
Age Scaled Score	11.0 (7–17)	12.5 (11–15)	10.0[a] (7–12)
Visual Recall	24.0 (13–33)	22.3 (10–34)	15.5[a] (8–33)
Verbal Recall	13.0 (8–16)	13.0 (11–16)	8.00[a] (5–10)
Verbal Learning	58.0 (41–63)	69.0 (49–71)	36.0[a] (34–43)
Verbal Fluency	52.0 (25–56)	57.5 (39–60)	34.5 (10–66)
Trailmaking Part A	16.0 (10–42)	19.0 (12–30)	36.5 (12–55)
Part B	35.0 (20–68)	37.5 (32–65)	67.5 (28–154)
Pegboard Dominant	51.0 (42–83)	65.5 (63–77)	89.5[a] (79–140)
Non-Dominant	64.0 (44–89)	73.5 (64–78)	102.0[a] (84–124)
NPZ-8	.25 (−.6–1.0)	.30 (−.3–.8)	−.78[a] (−1.9–.2)

Note. Testing was as described in text. Values (except N) are mean (range).
[a]Impaired significantly different from unimpaired ($p < .05$, two-tailed, Mann-Whitney *U* test).

Table 3 [^{11}C](***R***)-PK11195 binding potential

	NC	*HIV+ (NI)*	*HIV+ (I)*
Anterior cingulate gyrus	0.042 ± 0.066	0.002 ± 0.054	0.077 ± 0.071
Basal ganglia	0.037 ± 0.033	0.146 ± 0.137	0.145 ± 0.076
Cerebellum	0.028 ± 0.098	0.082 ± 0.071	0.104 ± 0.097
Frontal cortex	0.033 ± 0.055	0.041 ± 0.102	0.068 ± 0.082
Lateral temporal cortex	0.044 ± 0.020	0.065 ± 0.065	0.070 ± 0.036
Mesial temporal cortex	0.021 ± 0.030	0.040 ± 0.061	0.018 ± 0.051
Occipital Cortex	0.167 ± 0.041	0.102 ± 0.109	0.178 ± 0.073
Pons	0.196 ± 0.059	0.169 ± 0.144	0.279 ± 0.078
Subcortical white matter	−0.058 ± 0.015	−0.028 ± 0.065	−0.012 ± 0.100
Thalamus	0.206 ± 0.068	0.368 ± 0.225	0.260 ± 0.092

Regional [^{11}C](***R***)-PK11195 binding potential (BP) values determined by cluster analysis and the simplified reference tissue model (SRTM) for normal control (NC), nonimpaired HIV-positive (HIV+ (NI)), and cognitively impaired HIV-positive (HIV+ (I)) subject groups.

therapy, it is not clear if our findings would pertain to nontreated subjects. HIV-infected subjects demonstrated a variety of minor MR imaging abnormalities. Constellations of these abnormalities (e.g., cortical atrophy, caudate atrophy, white matter hyperintensities) have been described in encephalopathic HIV-infected individuals (see Paul *et al* [2002] for review). Caudate atrophy has been most commonly associated with cognitive dysfunction along with cortical atrophy and white matter hyperintensities; however, the literature does not support a strong relationship between cortical atrophy or white matter abnormalities and cognitive dysfunction. In our small study, even with contrast administration, MRI features did not unambiguously discriminate between neurocognitively impaired and nonimpaired individuals. The inability to distinguish impaired and nonimpaired individuals suggests that the physiological abnormalities of subtle neurocognitive impairment in HIV infection do not have prominent structural correlates detectable by contrast enhanced MRI. Other MR techniques such as MR spectroscopy (Brack-Werner, 1999; Navia, 1997) for neuronal markers such as *N*-acetylaspartate or diffusion tensor imaging (Filippi *et al*, 2001; Pomara *et al*, 2001) may be more sensitive in detecting abnormalities associated with these subtle cognitive abnormalities.

Given that brain structural changes would be expected to be a late and insensitive means of detecting physiological changes, we utilized PET to detect neuroinflammatory changes potentially associated with HIV infection. PET has been used extensively in HIV-infected individuals. Most PET studies have focused on the use of [^{18}F]FDG to discriminate infectious or neoplastic lesions (Heald *et al*, 1996; O'Doherty *et al*, 1997; Palestro and Torres, 1999). Some have used [^{18}F]FDG PET to assess neurocognitive deficits in HIV-infected subjects (Goodkin *et al*, 1997) and although the findings have not been robust, there is some suggestion that hypometabolism in the cortex and hypermetabolism in the striatum are associated with cognitive impairment in adults (Arendt, 1995; Brunetti *et al*, 1989; Rottenberg *et al*, 1996), but the opposite pattern was seen in children (Depas *et al*, 1995).

Because both *in vitro* and *in vivo* studies have shown that microglia express a high concentration of PBR binding sites, the PBR ligand PK11195 has been used in a variety of studies to investigate macrophage infiltration in the CNS of animal models and human diseases (Banati, 2002; Cagnin *et al*, 2002; Debruyne *et al*, 2003; Kadota *et al*, 1996; Petit-Taboue *et al*, 1991; Vowinckel *et al*, 1997; Yamagishi and Kawaguchi, 1998). The low abundance of PBR in the unperturbed CNS (Banati *et al*, 1997; Benavides *et al*, 1988) contrasts with the abundance of binding detected in brains with a variety of neuroinflammatory

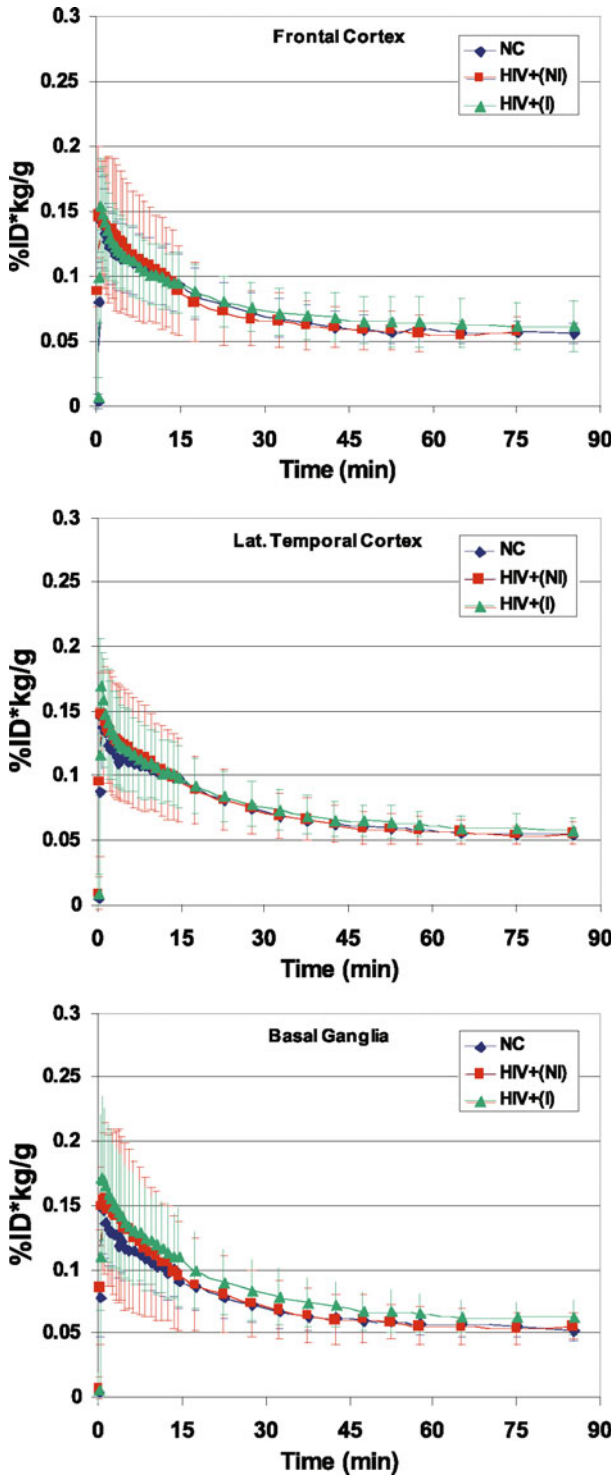

Figure 1 [^{11}C](***R***)-PK11195 retention in the brains of HIV-infected humans with and without neurocognitive impairment. Average group time activity curves (±1 SD) for frontal cortex, lateral temporal cortex, and basal ganglia following the injection [^{11}C](***R***)-PK–11195 for normal control (NC), HIV-infected neurocognitively non-impaired (HIV+ (NI)), and HIV-infected neurocognitively impaired (HIV+ (I)) groups. Although some regional variation in the retention characteristics were observed, no discernible component of specific binding was observed in any brain region in impaired HIV-infected subjects as compared to noninfected HIV subjects or seronegative controls.

diseases (Banati *et al*, 1997; Debruyne *et al*, 2003). Human studies of multiple sclerosis and Alzheimer's disease have reported good concordance between PK11195 binding in the CNS and regions of neuroinflammation. Because immunosuppressive lentiviral encephalitides are characterized by a prominent macrophage infiltration, these diseases might also be amenable to PET [^{11}C](***R***)-PK11195 assessment.

In the course of preparing this paper, a similar study examining five non–HIV-infected and 10 HIV-infected subjects was published by Hammoud *et al* (2005). These investigators reported, "patients with HAD showed significantly higher [^{11}C]-(***R***)-PK11195 binding than controls in five out of 8 brain regions." However, "non-demented HIV+ patients did not show significantly increased binding compared to controls" and nondemented and demented HIV-infected subjects did not show significant differences in binding. Differences in our current report and that of Hammoud and colleagues may in part be due to differences in data analysis. To reach the above conclusions, these investigators compared mean regional activity normalized to the mean activity in white matter. To better compare our results to the previous study, we performed a similar analysis based on normalized data (Table 4). Paradoxically, using this type of analysis, three regions (mesial temporal cortex, occipital cortex, and pons) showed higher binding in our noninfected controls than in the infected subjects (regardless of impairment).

Another reason for differences in the studies may be due to differences in the control populations. Although regions of interest may not be precisely defined the same in the two studies, five regions could be compared between the two studies (frontal cortex, occipital cortex, thalamus, pons, and cerebellum). In three regions (frontal cortex, occipital cortex and cerebellum), the mean normalized binding in Hammoud's controls was substantially lower then our controls. Because it is more difficult to compare the different groups of affected subjects in the two studies, we performed a similar analysis comparing our noninfected controls to impaired and nonimpaired HIV-infected subjects.

Like our study, the Hammoud *et al* study was not able to distinguish impaired from nonimpaired HIV-infected subjects. Because PET studies are expensive and logistically complex, both the previously published study and ours suffer from small numbers of subjects. We performed a meta-analysis by combining our findings with those of Hammoud *et al*. Although we were able to detect differences between our controls (see above), comparison of the combined impaired and nonimpaired HIV-infected subjects showed no significant difference. Given the small differences between binding potentials of impaired and nonimpaired subjects, power analyses suggest that a PET PK study would have to contain approximately 100 subjects to show a statistically

Table 4 Normalized [^{11}C](***R***)-PK11195 radioactivity

	NC	*HIV+ (NI)*	*HIV+ (I)*
Anterior cingulate gyrus	1.456 ± 0.149	1.365 ± 0.115	1.231 ± 0.158
Basal ganglia	1.136 ± 0.149	1.332 ± 0.119	1.393 ± 0.222
Cerebellum	1.528 ± 0.097	1.426 ± 0.156	1.331 ± 0.173
Frontal cortex	1.414 ± 0.158	1.333 ± 0.125	1.247 ± 0.190
Lateral temporal cortex	1.458 ± 0.119	1.351 ± 0.129	1.287 ± 0.137
Mesial temporal cortex*	1.392 ± 0.110	1.257 ± 0.087	1.219 ± 0.118
Occipital Cortex*	1.581 ± 0.124	1.481 ± 0.113	1.300 ± 0.195
Pons*	1.587 ± 0.189	1.522 ± 0.010	1.304 ± 0.228
Subcortical white matter	1.000 ± 0.000	1.000 ± 0.000	1.000 ± 0.000
Thalamus	1.746 ± 0.180	1.605 ± 0.122	1.625 ± 0.260

Regional [^{11}C](***R***)-PK11195 activity averaged from 10 to 60 min postinjection, normalized to the mean activity in white matter. Normal control (NC), nonimpaired HIV-positive (HIV+ (NI)), and cognitively impaired HIV-positive (HIV+ (I)) subject groups. *Significantly different from control ($P < .05$, Mann-Whitney U test).

significant difference between impaired and nonimpaired subjects. This draws into question the utility of [^{11}C](***R***)-PK11195 PET in studies of minor cognitive impairment in HIV infection and certainly obviates its utility in evaluation of individual patients.

To optimize our PET sensitivity, we used the ***R***-enantiomer of PK11195 to afford higher affinity for these studies. Our previous PET study of simian immunodeficiency virus (SIV)-infected macaques (Venneti *et al*, 2004) demonstrated proof of principle that [^{11}C](***R***)-PK11195 can detect neuroinflammation associated with lentiviral encephalitis. However, the animal model used for these studies employed CD8 T-cell depletion and led to severe lentiviral encephalitis with potential significant differences in severity of macrophage aggregation compared to the human disease. In the previous simian study, we found increased PK11195 binding potential without change in dissociation constant in macaques with severe SIV encephalitis. Obviously clinical pathological correlations are more limited in human studies. For numerous reasons it is difficult to obtain elaborate human clinical testing in the premorbid time period. Therefore clinical pathological correlations frequently have lengthy time gaps between performing a test and the demise of the patient and neuropathological correlation. Because AIDS dementia occurs in the terminal stages of infection, it has been possible to draw a fairly close correlation between AIDS dementia and HIV encephalitis (Achim *et al*, 1994; Glass *et al*, 1995). Unfortunately we currently have no data on what PET [^{11}C](***R***)-PK11195 studies would show in profoundly demented HIV-infected patients with HIV encephalitis. We have, however, attempted to make this correlation using the SIV model (Venneti *et al*, 2004). Treatment of HIV infection also interjects an additional complexity into the human studies. Because HIV is known to enter the CNS early after infection, it is possible that damage and microglial activation could occur and enter various stages of resolution. If this were the case in our subjects, our negative findings indicate that such lesions are not readily detected by [^{11}C](***R***)-PK11195.

In analogy to our study, a recent report at the International Congress on Alzheimer's Disease and Related Disorders (ICAD) demonstrated that in six patients with mild cognitive impairment (a potential precursor to Alzheimer's disease), [^{11}C]PK11195 PET showed no increase binding potential compared to five age- and sex-matched controls (Schuitemaker *et al*, 2004). If [^{11}C](***R***)-PK11195 PET is assumed to be a sensitive marker of microglial activation, then our finding in HIV-infected subjects and Shuitemaker *et al*'s finding in elderly subjects suggest that mild cognitive impairment in both diseases is independent of microglia. Alternatively, more sensitive probes are necessary to study a more modest macrophage activation associated with early phases of this disease.

A spectrum of neurocognitive abnormalities have been described in HIV-infected individuals, ranging from minor motor and cognitive abnormalities to frank dementia. The pathological substrate of HIV-dementia has been shown to be HIV encephalitis, a peculiar form of encephalitis characterized by an abundance of activated macrophages in the CNS. The relationship between minor cognitive abnormalities and dementia has not been fully elucidated; however, it is logical to assume that dementia must begin with more subtle cognitive abnormalities that progress to greater severity and thus dementia. If the minor neurocognitive abnormalities associated with HIV infection were on the pathological continuum to HIV dementia, then it might represent an early stage of macrophage activation. PET studies are logistically difficult and financially challenging so it is important to recognize that our inability to distinguish impaired from nonimpaired subjects may in part be due to the limited number of subjects. That we did not detect a difference in either the [^{11}C](***R***)-PK11195 concentration time-activity curves or binging potential in impaired versus non-impaired individuals suggests that either PET scanning with [^{11}C](***R***)-PK11195 lacks the sensitivity to detect this early or that the pathological substrate of minor cognitive and motor impairment is not an early form of lentiviral encephalitis.

Methods

Subjects

This study was reviewed and approved by the University of Pittsburgh Institutional Review Board.

Subjects were recruited from the ongoing Allegheny County Neuropsychiatric Survey and had undergone an intensive neuropsychological evaluation within six months of entry into the present study. All subjects received an intensive neuropsychological evaluation within 6 months of study entry. This broad assessment of cognitive function permitted a qualitative analysis of neuropsychological impairment in HIV seropositive individuals (Becker *et al*, 1997). Each participant underwent a semistructured psychosocial interview, and completed questionnaires concerning psychiatric symptomatology. Subjects completed screening questions concerning new episodes of mood or anxiety disorders, psychosis, and substance abuse/dependence. Subclinical psychiatric symptoms were assessed with the Brief Symptom Inventory, and the Neuropsychiatric Inventory. The data from the neurobehavioral evaluation were reviewed by a neuropsychologist (Dr. Becker) and a neurologist (Dr. Lopez) who were blinded to the results of the PET and MR imaging study. The determination of the presence of cognitive impairment was based on the results of the test battery. A subject was considered to be impaired if they had abnormal performance in two cognitive domains. Impaired performance within a domain occurred when the patient had scores on two tests that were more than 1.5 standard deviation units below the level expected based on age and education level.

After subjects consented to participate in the study, all testing was coded to a study number to maintain anonymity and assure blinded data analyses. Prior to undergoing an MRI scan an intravenous catheter was placed and blood drawn for CD4 white count analysis and plasma viral load assessment.

Magnetic resonance imaging

Magnetic resonance (MR) imaging was performed using a 1.5-Tesla whole-body MR scanner (General Electric Medical Systems, Milwaukee, WI). The standard quadrature, birdcage head coil was used for scanning the subjects, placed supine on the imaging table. Data acquisition was performed using a protocol of standard imaging sequences to evaluate anatomical detail, followed by the acquisition of a high-resolution gradient echo data set to be used for MRI PET co-registration and a dynamic, contrast-enhanced echo planar imaging acquisition.

Three-dimensional spoiled gradient-recalled (SPGR) images were acquired in the coronal plane with a field of view of 24 cm and an effective resolution of $.9 \times .9 \times 1$ mm^3 prior to contrast injection to provide a high-resolution data set for MRI-PET coregistration. Volume measurements were determined as described before using a semiautomated segmentation algorithm (MORPH) software (Joe *et al*, 1999; Johnson *et al*, 1993).

The MRI examinations were evaluated by a board-certified neuroradiologist (Dr. Meltzer), blinded to CD4 T-cell count, neuropsychological test results, and all other clinical information except for the diagnosis of HIV-infection and subject age. The images were viewed on a monitor, and visually evaluated for the presence of findings consistent with HIV encephalopathy, including (1) cerebral volume loss greater than expected for age; (2) disproportionate ventricular enlargement; and (3) confluent, symmetric periventricular white matter hyperintensities.

[^{11}C]($\boldsymbol{R}$)-PK11195 radiosynthesis

High specific activity [^{11}C]($\boldsymbol{R}$)-PK11195 was produced at the University of Pittsburgh Medical Center PET Facility using methods similar to those previously described by the Hammersmith PET Group (Shah *et al*, 1994), except that the methylation was performed at room temperature for 2 min to minimize the dechlorination side reaction (Cleij *et al*, 2003). Chemical and radiochemical purities were $\geq 95\%$ with specific activities $\geq$2.0 Ci/μmol at the end of a 40-min synthesis.

PET imaging

All PET data were acquired in three-dimensional imaging mode using an ECAT HR+ PET scanner (CTI PET Systems, Knoxville, TN). Prior to radiotracer injection, a 10- to 15-min transmission scan was performed using rotating ^{68}Ga/^{68}Ge rod sources for the purpose of attenuation correction of emission data. Immediately following the transmission scan, patients were injected with 12 mCi of [^{15}O]H_2O and a 5-min (4-frame) PET scan was acquired. After a 15-min delay to allow for the decay of oxygen-15, subjects were injected intravenously over 30 s with approximately 15 mCi (average dose 14.3 ± 1.0 mCi, range 13.0 to 15.8 mCi) of high specific activity [^{11}C]($\boldsymbol{R}$)-PK11195 in 5 ml of sterile isotonic saline. A dynamic series of PET scans was acquired over 90 min in 33 frames, commencing at the start of radiotracer injection. Images were reconstructed using Fourier rebinning and two-dimensional filtered backprojection using a 4-mm Hanning filter. Emission data were corrected for attenuation, dead time, scatter, and radioactive decay.

Data analysis

PET scans of each subject were centered using the algorithm of Minoshima *et al* (1992) and coregistered to the subject's corresponding [^{15}O]H_2O scan using the Automated Image Registration (AIR) algorithm (Woods *et al*, 1992). MR images were aligned to the [^{15}O]H_2O scan and resliced using AIR (Woods *et al*, 1993) to yield MR images in the same spatial orientation as the and [^{11}C]($\boldsymbol{R}$)-PK11195 PET images. The [^{15}O]H_2O PET image was chosen as the target for the MR to PET image registration due to the greater degree

of anatomical detail in brain compared to the [^{11}C](***R***)-PK11195 PET image. Both PET to PET and PET to MR image registrations were checked for accuracy by comparing anatomical landmarks in an orthogonal image viewer. Regions of interest (ROIs) were defined on multiple contiguous planes on the coregistered MR image using standard anatomical criteria established in our laboratory (Meltzer *et al*, 1998) and applied to the dynamic PET images to generate time-activity curves for the anterior cingulate gyrus (ANC), basal ganglia (BSG), cerebellum (CER), midfrontal cortex (FRC), lateral temporal cortex (LTC), mesial temporal cortex (MTC), occipital cortex (OCC), pons (PON), subcortical white matter (SWM), and thalamus (THL). The regional brain radioactivity concentrations per gram of brain tissue were normalized to both the injected dose of [^{11}C](***R***)-PK11195 and the body mass of the subject in kilograms (%ID*kg)/g.

Because HIVD is characterized by widespread and unpredictable patterns of pathologic involvement, it is not possible to anatomically define a consistent reference tissue which is free of disease pathology within a study cohort. For this reason, a cluster analysis technique was employed to segment the dynamic PET image data on a voxel-by-voxel basis into "clusters" of voxels with indistinguishable ligand kinetics without any anatomical restriction. From these clusters, it is possible to extract a normal ligand kinetic that is representative of *in vivo* free and nonspecific ligand kinetics. This normal ligand kinetic can be used as a reference input function for image-based methods of analysis of radiotracer binding such as the simplified reference tissue model (Gunn *et al*, 1997; Lammertsma and Hume, 1996).

To determine the regional binding of [^{11}C](***R***)-PK11195, a basis function implementation of the simplified reference tissue model (SRTM) was applied to the dynamic PET image data (Gunn *et al*, 1997; Lammertsma and Hume, 1996). This method of analysis relies on the definition of an anatomic "reference tissue," which is devoid of specific radioligand binding to estimate three parameters: R_I (the ratio of radiotracer delivery between target and reference tissue); k_2 (the efflux rate constant from the target tissue); and the binding potential (BP), which is a measure of specifically bound radioligand. For many widely used neuroreceptor radioligands, such as the carbon-11–labeled dopamine D2 receptor antagonist [^{11}C]raclopride, the cerebellum provides a suitable reference ligand kinetic that does not contain a significant component of specific binding. In this study, the reference tissue is defined by the cluster that was most representative of the normal ligand kinetic as determined in non–HIV-infected control subjects ($n = 3$).

A second technique employed for the analysis of regional [^{11}C](***R***)-PK11195 PET data uses a white matter ROI as a reference value to normalize radiotracer binding in other regions, as recently described by Hammoud *et al*, (2005). This simplified image-derived method was investigated as a potential alternative to cluster analysis and SRTM. Regional PET time- activity data were summed over the 10 to 60-min postinjection interval to obtain an index of radiotracer concentration. For cortical and subcortical gray matter regions, this index was normalized to that obtained from the white matter.

Statistical analysis

Student's *t* tests for unequal variances was used to compare the CD4 count by viral load. Fisher's Exact statistic was used to compare the rate of structural abnormalities among those with and without neurocognitive impairment. One-way analysis of variance (ANOVA) test were used to compare the neuropsychological test scores between impaired and unimpaired patients and the binding potential in various regions among the unimpaired, HIV infected, and HIV noninfected. A two-sample *t* test was used to compare the normalized binding potential between normal controls from this study with normal controls from a previously reported study.

Reference

Achim CL, Wang R, Miners DK, Wiley CA (1994). Brain viral burden in HIV-infection. *J Neuropathol Exp Neurol* **53:** 284–294.

Arendt G (1995). Imaging methods as a diagnostic tool in neuro-AIDS. A review. *Bildgebung* **62:** 310–319.

Avison MJ, Nath A, Berger JR (2002). Understanding pathogenesis and treatment of HIV dementia: a role for magnetic resonance? *Trends Neurosci* **25:** 468–473.

Aylward EH, Henderer JD, McArthur JC, Brettschneider PD, Harris GJ, Barta PE, Pearlson GD (1993). Reduced basal ganglia volume in HIV-1-associated dementia: results from quantitative neuroimaging. *Neurology* **43:** 2099–2104.

Banati RB (2002). Visualising microglial activation in vivo. *Glia* **40:** 206–217.

Banati RB, Goerres GW, Myers R, Gunn RN, Turkheimer FE, Kreutzberg GW, Brooks DJ, Jones T, Duncan JS (1999). [11C](R)-PK11195 positron emission tomography imaging of activated microglia in vivo in Rasmussen's encephalitis. *Neurology* **53:** 2199–2203.

Banati RB, Myers R, Kreutzberg GW (1997). PK ('peripheral benzodiazepine')–binding sites in the CNS indicate early and discrete brain lesions: microautoradiographic detection of [3H]PK11195 binding to activated microglia. *J Neurocytol* **26:** 77–82.

Banati RB, Newcombe J, Gunn RN, Cagnin A, Turkheimer F, Heppner F, Price G, Wegner F, Giovannoni G, Miller DH, Perkin GD, Smith T, Hewson AK, Bydder G, Kreutzberg GW, Jones T, Cuzner ML, Myers R (2000). The peripheral benzodiazepine binding site in the brain in multiple

sclerosis: quantitative in vivo imaging of microglia as a measure of disease activity. *Brain* **123** (Pt 11): 2321–2337.

Becker JT, Sanchez J, Dew MA, Lopez OL, Dorst SK, Banks G (1997). Neuropsychological abnormalities among HIV-infected individuals in a community-based sample. *Neuropsychology* **11:** 592–601.

Benavides J, Cornu P, Dennis T, Dubois A, Hauw JJ, MacKenzie ET, Sazdovitch V, Scatton B (1988). Imaging of human brain lesions with an omega 3 site radioligand. *Ann Neurol* **24:** 708–712.

Brack-Werner R (1999). Astrocytes: HIV cellular reservoirs and important participants in neuropathogenesis. *AIDS* **13:** 1–22.

Broderick D, Wippold F, Clifford D, Kido D, Wilson B (1993). White matter lesions and cerebral atrophy on MR images in patients with and without AIDS dementia complex. *Am J Roentgenol* **161:** 177–181.

Brunetti A, Berg G, Di Chiro G, Cohen RM, Yarchoan R, Pizzo PA, Broder S, Eddy J, Fulham MJ, Finn RD, et al (1989). Reversal of brain metabolic abnormalities following treatment of AIDS dementia complex with 3′-azido-2′, 3′-dideoxythymidine (AZT, zidovudine): a PET-FDG study. *J Nucl Med* **30:** 581–590.

Budka H (1991). Neuropathology of human immunodeficiency virus infection. *Brain Pathology* **1:** 163–175.

Cagnin A, Brooks DJ, Kennedy AM, Gunn RN, Myers R, Turkheimer FE, Jones T, Banati RB (2001a). In-vivo measurement of activated microglia in dementia. *Lancet* **358:** 461–467.

Cagnin A, Gerhard A, Banati RB (2002). In vivo imaging of neuroinflammation. *Eur Neuropsychopharmacol* **12:** 581–586.

Cagnin A, Myers R, Gunn RN, Lawrence AD, Stevens T, Kreutzberg GW, Jones T, Banati RB (2001b). In vivo visualization of activated glia by [11C] (R)-PK11195-PET following herpes encephalitis reveals projected neuronal damage beyond the primary focal lesion. *Brain* **124:** 2014–2027.

Chang L, Ernst T, Leonido-Yee M, Witt M, Speck O, Walot I, Miller EN (1999). Highly active antiretroviral therapy reverses brain metabolite abnormalities in mild HIV dementia. *Neurology* **53:** 782–789.

Cleij MC, Aigbirhio FI, Baron JC, Clark JC (2003). Base-promoted dechlorination of (R)-[C-11]PK-11195. *J Labeled Comp Radiopharm* **46 (Suppl. 1):** S-88.

Dal Pan GJ, McArthur JC (1996). Neuroepidemiology of HIV infection. *Neurologic Clin* **14:** 359–382.

Debruyne JC, Versijpt J, Van Laere KJ, De Vos F, Keppens J, Strijckmans K, Achten E, Slegers G, Dierckx RA, Korf J, De Reuck JL (2003). PET visualization of microglia in multiple sclerosis patients using [11C]PK11195. *Eur J Neurol* **10:** 257–264.

Depas G, Chiron C, Tardieu M, Nuttin C, Blanche S, Raynaud C, Syrota A (1995). Functional brain imaging in HIV-1-infected children born to seropositive mothers. *J Nucl Med* **36:** 2169–2174.

Di Sclafani V, Mackay RD, Meyerhoff DJ, Norman D, Weiner MW, Fein G (1997). Brain atrophy in HIV infection is more strongly associated with CDC clinical stage than with cognitive impairment. *J Int Neuropsychol Soc* **3:** 276–287.

Ernst T, Chang L, Arnold S (2003). Increased glial metabolites predict increased working memory network activation in HIV brain injury. *Neuroimage* **19:** 1686–1693.

Filippi CG, Ulug AM, Ryan E, Ferrando SJ, van Gorp W (2001). Diffusion tensor imaging of patients with HIV and normal-appearing white matter on MR images of the brain. *AJNR Am J Neuroradiol* **22:** 277–283.

Gerhard A, Banati RB, Goerres GB, Cagnin A, Myers R, Gunn RN, Turkheimer F, Good CD, Mathias CJ, Quinn N, Schwarz J, Brooks DJ (2003). [(11)C](R)-PK11195 PET imaging of microglial activation in multiple system atrophy. *Neurology* **61:** 686–689.

Glass JD, Fedor H, Wesselingh SL, McArthur JC (1995). Immunocytochemical quantitation of human immunodeficiency virus in the brain: correlations with dementia. *Ann Neurol* **38:** 755–762.

Goodkin K, Wilkie FL, Concha M, Asthana D, Shapshak P, Douyon R, Fujimura RK, LoPiccolo C (1997). Subtle neuropsychological impairment and minor cognitive-motor disorder in HIV-1 infection. Neuroradiological, neurophysiological, neuroimmunological, and virological correlates. *Neuroimag Clin N Am* **7:** 561–579.

Grant I, Heaton RK, Atkinson JH (1995). Neurocognitive disorders in HIV-1 infection. HNRC Group. HIV Neurobehavioral Research Center. *Curr Top Microbiol Immunol* **202:** 11–32.

Grassi MP, Clerici F, Boldorini R, Perin C, Vago L, D'Arminio Monforte A, Borella M, Nebuloni M, Mangoni A (1997). HIV encephalitis and HIV leukoencephalopathy are associated with distinct clinical and radiological subtypes of the AIDS dementia complex [letter]. *AIDS* **11:** 690–691.

Gunn RN, Lammertsma AA, Hume SP, Cunningham VJ (1997). Parametric imaging of ligand-receptor binding in PET using a simplified reference region model. *Neuroimage* **6:** 279–287.

Hammoud DA, Endres CJ, Chander AR, Guilarte TR, Wong DF, Sacktor NC, McArthur JC, Pomper MG (2005). Imaging glial cell activation with [11C]-R-PK11195 in patients with AIDS. *J Neurovirol* **11:** 346–355.

Harrison MJ, Newman SP, Hall-Craggs MA, Fowler CJ, Miller R, Kendall BE, Paley M, Wilkinson I, Sweeney B, Lunn S, Carter S, Williams I (1998). Evidence of CNS impairment in HIV infection: clinical, neuropsychological, EEG, and MRI/MRS study. *J Neurol Neurosurg Psychiatry* **65:** 301–307.

Heald AE, Hoffman JM, Bartlett JA, Waskin HA (1996). Differentiation of central nervous system lesions in AIDS patients using positron emission tomography (PET). *Int J STD AIDS* **7:** 337–346.

Joe BN, Fukui MB, Meltzer CC, Huang QS, Day RS, Greer PJ, Bozik ME (1999). Brain tumor volume measurement: comparison of manual and semiautomated methods. *Radiology* **212:** 811–816.

Johnson LA, Pearlman JD, Miller CA, Young TI, Thulborn KR (1993). MR quantification of cerebral ventricular volume using a semiautomated algorithm. *AJNR Am J Neuroradiol* **14:** 1373–1378.

Kadota Y, Inoue K, Tokunaga R, Taketani S (1996). Induction of peripheral-type benzodiazepine receptors in mouse brain following thioacetamide-induced acute liver failure. *Life Sciences* **58:** 953–959.

Kaul M, Garden GA, Lipton SA (2001). Pathways to neuronal injury and apoptosis in HIV-associated dementia. *Nature* **410:** 988–994.

Lammertsma AA, Hume SP (1996). Simplified reference tissue model for PET receptor studies. *Neuroimage* **4:** 153–158.

Lexa F (1994). Neuroradiological manifestations of acquired immunodeficiency syndrome. *Sem Roentgen* **29:** 288–302.

Masliah E, Achim CL, Ge N, De Teresa R, Terry RD, Wiley CA (1992). Spectrum of human immunodeficiency virus-associated neocortical damage. *Ann Neurol* **32:** 321–329.

McArthur JC, Haughey N, Gartner S, Conant K, Pardo C, Nath A, Sacktor N (2003). Human immunodeficiency virus-associated dementia: an evolving disease. *J NeuroVirol* **9:** 205–221.

McArthur JC, Kumar AJ, Johnson DW, Selnes OA, Becker JT, Herman C, Cohen BA, Saah A (1990). Incidental white matter hyperintensities on magnetic resonance imaging in HIV-1 infection. Multicenter AIDS Cohort Study. *J Acquir Immune Defic Syndr* **3:** 252–259.

Meltzer CC, Smith G, Price JC, Reynolds CF, 3rd, Mathis CA, Greer P, Lopresti B, Mintun MA, Pollock BG, Ben-Eliezer D, Cantwell MN, Kaye W, DeKosky ST (1998). Reduced binding of [18F]altanserin to serotonin type 2A receptors in aging: persistence of effect after partial volume correction. *Brain Res* **813:** 167–171.

Minoshima S, Berger KL, Lee KS, Mintun MA (1992). An automated method for rotational correction and centering of three-dimensional functional brain images. *J Nucl Med* **33:** 1579–1585.

Navia BA (1997). Clinical and biologic features of the AIDS dementia complex. *Neuroimag Clin N Am* **7:** 581–592.

O'Doherty MJ, Barrington SF, Campbell M, Lowe J, Bradbeer CS (1997). PET scanning and the human immunodeficiency virus-positive patient. *J Nucl Med* **38:** 1575–1583.

Olsen W, Longo F, Mills C, Norman D (1988). White matter disease in AIDS: findings at MR imaging. *Radiology* **169:** 445–448.

Ouchi Y, Yoshikawa E, Sekine Y, Futatsubashi M, Kanno T, Ogusu T, Torizuka T (2005). Microglial activation and dopamine terminal loss in early Parkinson's disease. *Ann Neurol* **57:** 168–175.

Palestro CJ, Torres MA (1999). Radionuclide imaging of nonosseous infection. *Q J Nucl Med* **43:** 46–60.

Pascal S, Resnick L, Barker WW, Loewenstein D, Yoshii F, Chang JY, Boothe T, Sheldon J, Duara R (1991). Metabolic asymmetries in asymptomatic HIV-1 seropositive subjects: relationship to disease onset and MRI findings. *J Nuc Med* **32:** 1725–1729.

Patel SH, Kolson DL, Glosser G, Matozzo I, Ge Y, Babb JS, Mannon LJ, Grossman RI (2002). Correlation between percentage of brain parenchymal volume and neurocognitive performance in HIV-infected patients. *AJNR: Am J Neuroradiol* **23:** 543–549.

Paul R, Cohen R, Navia B, Tashima K (2002). Relationships between cognition and structural neuroimaging findings in adults with human immunodeficiency virus type-1. *Neurosci Biobehav Rev* **26:** 353–359.

Petit-Taboue MC, Baron JC, Barre L, Travere JM, Speckel D, Camsonne R, MacKenzie ET (1991). Brain kinetics and specific binding of [11C]PK 11195 to omega 3 sites in baboons: positron emission tomography study. *Eur J Pharmacol* **200:** 347–351.

Pomara N, Crandall DT, Choi SJ, Johnson G, Lim KO (2001). White matter abnormalities in HIV-1 infection: a diffusion tensor imaging study. *Psychiatry Res* **106:** 15–24.

Post MJ, Levin BE, Berger JR, Duncan R, Quencer RM, Calabro G (1992). Sequential cranial MR findings of asymptomatic and neurologically symptomatic HIV+ subjects. *AJNR: Am J Neuroradiol* **13:** 359–370.

Post MJ, Tate LG, Quencer RM, Hensley GT, Berger JR, Sheremata WA, Maul G (1988). CT, MR, and pathology in HIV encephalitis and meningitis. *AJR* **151:** 373–380.

Raghavendra Rao VL, Dogan A, Bowen KK, Dempsey RJ (2000). Traumatic brain injury leads to increased expression of peripheral-type benzodiazepine receptors, neuronal death, and activation of astrocytes and microglia in rat thalamus. *Exp Neurol* **161:** 102–114.

Raininko R, Elovaara I, Virta A, Valanne L, Haltia M, Valle SL (1992). Radiological study of the brain at various stages of human immunodeficiency virus infection: early development of brain atrophy. *Neuroradiology* **34:** 190–196.

Rosci MA, Pigorini F, Bernabei A, Pau FM, Volpini V, Merigliano DE, Meligrana MF (1992). Methods for detecting early signs of AIDS dementia complex in asymptomatic HIV-1-infected subjects. *AIDS* **6:** 1309–1316.

Rottenberg DA, Sidtis JJ, Strother SC, Schaper KA, Anderson JR, Nelson MJ, Price RW (1996). Abnormal cerebral glucose metabolism in HIV-1 seropositive subjects with and without dementia. *J Nucl Med* **37:** 1133–1141.

Schuitemaker A, van Berckel BN, Kropholler M, Boellaard R, Jonker C, Scheltens P, Lammerstma AA (2004). Microglia activation in mild cognitive impairment. *Neurobiol Aging* **25:** 286.

Shah F, Hume SP, Pike VW, Ashworth S, McDermott J (1994). Synthesis of the enantiomers of [N-methyl-11C]PK 11195 and comparison of their behaviours as radioligands for PK binding sites in rats. *Nucl Med Biol* **21:** 573–581.

Sonnerborg A, Saaf J, Alexius B, Strannegard O, Wahlund LO, Wetterberg L (1990). Quantitative detection of brain aberrations in human immunodeficiency virus type 1-infected individuals by magnetic resonance imaging. *J Infect Dis* **162:** 1245–1251.

Stephenson DT, Schober DA, Smalstig EB, Mincy RE, Gehlert DR, Clemens JA (1995). Peripheral benzodiazepine receptors are colocalized with activated microglia following transient global forebrain ischemia in the rat. *J Neurosci* **15:** 5263–5274.

Venneti S, Lopresti BJ, Wang G, Bissel SJ, Mathis CA, Meltzer CC, Boada F, Capuano S, 3rd, Kress GJ, Davis DK, Ruszkiewicz J, Reynolds IJ, Murphey-Corb M, Trichel AM, Wisniewski SR, Wiley CA (2004). PET imaging of brain macrophages using the peripheral benzodiazepine receptor in a macaque model of neuroAIDS. *J Clin Invest* **113:** 981–989.

Vowinckel E, Reutens D, Becher B, Verge G, Evans A, Owens T, Antel JP (1997). PK11195 binding to the peripheral benzodiazepine receptor as a marker of microglia activation in multiple sclerosis and experimental autoimmune encephalomyelitis. *J Neurosc Res* **50:** 345–353.

Wenserski F, von Giesen HJ, Wittsack HJ, Aulich A, Arendt G (2003). Human immunodeficiency virus 1-associated minor motor disorders: perfusion-weighted MR imaging and H MR spectroscopy. *Radiology* **228:** 185–192.

Wiley C, Masliah E, Morey M, Lemere C, DeTeresa RM, Grafe MR, Hansen LA, Terry RD (1991). Neocortical damage during HIV infection. *AnnNeurol* **29:** 651–657.

Woods RP, Cherry SR, Mazziotta JC (1992). Rapid automated algorithm for aligning and reslicing PET images. *J Comput Assist Tomogr* **16:** 620–633.

Woods RP, Mazziotta JC, Cherry SR (1993). MRI-PET registration with automated algorithm. *J Comput Assist Tomogr* **17:** 536–546.

Yamagishi H, Kawaguchi M (1998). Characterization of central- and peripheral-type benzodiazepine receptors in rat salivary glands. *Biochem Pharmacol* **55:** 209–214.